Cancer Nanotechnology

RESEARCH Open Access

Anticancer platinum-drug delivered by mesenchymal stromal cells improves its activity on glioblastoma

Valentina Coccè[1†], Eleonora Martegani[1†], Luisa Doneda[1], Isabella Rimoldi[2*], Giorgio Facchetti[2*], Coffetti Giulia[2], Giorgio Lucchini[3], Leda Roncoroni[4,5], Aldo Giannì[1,6], Costantino Corradini[7], Giulio Alessandri[1], Emilio Ciusani[8,9], Francesco Cilurzo[2], Silvia Franzè[2], Francesca Paino[1†] and Augusto Pessina[1†]

†Valentina Coccè and Eleonora Martegani have contributed equal first name.

†Francesca Paino and Augusto Pessina have contributed equal last name.

*Correspondence: isabella.rimoldi@unimi.it; giorgio.facchetti@unimi.it

[2] CRC StaMeTec, Department of Pharmaceutical Science, University of Milan, Via Mangiagalli 25, 20133 Milan, Italy
Full list of author information is available at the end of the article

Abstract

Background: Glioblastoma multiforme (GBM) is nowadays the most aggressive tumor affecting brain in adults with a very poor prognosis due to the limited therapies and the systemic cytotoxicity. Among the different new drugs, recently has been reported the in vitro anti-glioma activity of a new cationic platinum(II) complex bearing 8-aminoquinoline as chelating ligand (Pt-8AQ). The purpose of this research work was to confirm the activity of Pt-8AQ on U87-GM spheroid and to investigate the ability of Mesenchymal Stromal Cells (MSCs) to incorporate and release Pt-8AQ in its active form. The MSCs were primed with Pt-8AQ under optimized conditions and the secretome was analyzed for evaluating the cytotoxic activity of Pt-8AQ and the presence of Extracellular Vesicles (Evs).

Results: The principal results showed that Pt-8AQ incorporated by MSCs was released in the secretome and exerted a significant higher anticancer activity with respect to the free drug. The release of Pt-8AQ did not occur in Evs, as demonstrated for other drugs, but it could be delivered bound to some specific carriers able to enhance its bioavailability and efficacy. Some hypotheses are discussed to explain this surprisingly finding out that, however, it needs more investigations.

Conclusions: The major conclusions are that cell mediated drug delivery systems could provide a potential approach to facilitate the GBM therapy by intratumoral administration of cells loaded with Pt-8AQ, being MSCs able to integrate it into the tumor mass and exert high therapeutic efficacy in situ. The increased efficacy of Pt-8AQ delivered by MSCs even suggests to deeper investigate a possible direct use of MSCs secretome both in situ and/or by systemic administration, being secretome able to pass the blood–brain tumor.

Keywords: Mesenchymal stromal cells, Drug delivery, Extracellular vesicles, Platinum drugs, Spheroids, Glioblastoma

Introduction

Glioblastoma multiforme (GBM) is nowadays the most aggressive tumor affecting the central nervous system in adults. GBM accounts for 49.1% of all primary malignant brain tumors with an average survival estimated to be only 8 months (National Brain Tumor Society). (Alessandri et al. 1999; Galli et al. 2004; Eramo et al. 2006; Roberts et al. 2016; Lisa et al. 2020) Actually, the presence of the blood–brain barrier (BBB) contribute to limit the efficacy of the chemotherapy leading to an early treatment failure. (Singh et al. 2021; Damato et al. 2021; Lee 2016; Chernov et al. 2021) As recently suggested, Cisplatin (CisPt) could be a possible adjuvant therapy in gliomas (Wang et al. 2017) but we demonstrated even the important anti-glioma activity of a new cationic Pt(II) complex bearing 8-aminoquinoline as chelating ligand called Pt-8AQ. (Coccè et al. 2021; Rimoldi et al. 2018) As the standard chemotherapy for glioblastoma proved not conclusive and no effective therapeutic modalities have emerged, it should be of great interest to develop new approaches by applying innovative cell mediated drug delivery systems that could be able to introduce significant improvements in the GBM therapy, to enhance the efficacy of drugs and to reduce the side effects. A possible and promising approach for an innovative drug delivery system (Tan et al. 2015) relies on the use of the so-called "Trojan horses" system to induce cancer cell damage, as in the case of neutrophils (Hosseinalizadeh et al. 2022) or nano-doxorubicin-loaded monocytes (Nano-DOX-MC). (Wang et al. 2018) However, a pivotal role was played by the advanced materials as a powerful toolkit, with designed structure and property serving for targeted drug delivery. (Wu et al. 2023; Sancho-Albero et al. 2023) Being Pt-8AQ a molecule with a significant stability, higher than that of CisPt, this platinum complex could be a good candidate for a new selective advanced cell chemotherapy approach in combination with Mesenchymal Stromal cells (MSCs). (Pessina et al. 2015) Our studies have demonstrated that MSCs, derived from different tissues (bone marrow, adipose tissue and gingival papilla), are able to incorporate and deliver drugs without any genetic manipulation. (Bonomi et al. 2013; Cocce et al. 2017; Pessina et al. 2011; Coccè et al. 2017; Cordani et al. 2023) The drug loaded MSCs acquired an anti-tumor activity and resulted capable to release the drug in situ against tumor cells with some advantages indeed as an increasing in drug protection by degradation and an enhanced drug availability for cancer cells. In the present study, we confirmed that the anticancer activity of the Pt-8AQ is also exerted against U87-GM grown cells as 3D multicellular spheroids that mimics solid tumors. Furthermore, we found that adipose tissue MSCs were able to incorporate and then release Pt-8AQ in their secretome with an increased anticancer activity against U87-GM ,(Tran and Damaser 2015) even if © activity of secretome did not result to be associated with Extracellular Vesicles (Evs).

Results

Effect of Pt-8AQ on U87-MG spheroids

Pt-8AQ (5 and 20 μM) was tested for its ability to affect the in vitro 3D spheroid formation induced by glioblastoma cells (Fig. 1A–C).

The results evidenced that 5 μM of the drug produced a diameter reduction of the spheroids at 6 days, if compared with control ones. Dosages of 20 μM completely

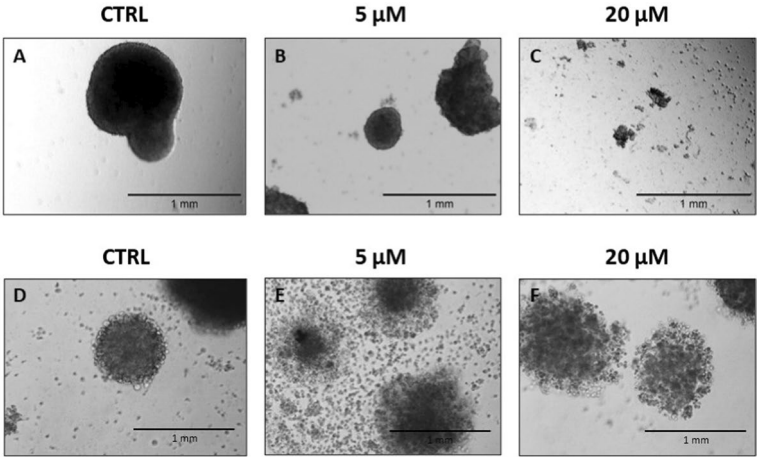

Fig. 1 Effect of Pt-8AQ on the formation of 3D U87-MG spheroids, and on pre-formed spheroids. Representative images of U87-MG spheroids after 6 days of culture (**A**, CTRL) or treated with Pt-8AQ (**B**, 5 µM or **C**, 20 µM) (40 ×magnification). Images **D**, **E** and **F** represent pre-formed spheroids treated 96 h with Pt-8AQ 5© **E** or 20 µM **F** compared to control spheroids **D**

inhibited the spheroid formation and only single cells or little cell aggregates were evidenced, probably attributed to the cells unable to growth as spheroids. The treatment for 96 h with 5 and 20 µM of Pt-8AQ on 6 days preformed U87-GM spheroids showed the presence of many detached single cells and an evident spheroid degradation (Fig. 1D–F).

The expression of pro-apoptotic gene was evaluated at 24 h after the treatment with 20 µM (Fig. 2A) and demonstrated a reduced expression of BCL-2 and BAX with an increase of PUMA and NOXA gene expression.

Interestingly, an identical profile expression of these genes was found when U87-GM cells were grown in 2D or 3D cultures (spheroids). A significant increase of the pro-apoptotic caspase-3 molecule was observed by RTq-PCR in the U87-GM cells treated for 24 h with Pt-8AQ 5 µM, also confirmed by detection of the enzymatic activity (Fig. 2B, C).

Sensitivity of mesenchymal stromal cells (MSCs) to Pt-8AQ

The sensitivity of MSCs to three increasing dosages (5, 10, and 20 µM) of Pt-8AQ was evaluated as cytotoxic effect at 24, 48 and 72 h. As reported in the histogram, the toxic effect evaluated on cell viability was dependent by both dosage and time of treatment. By expressing this effect as 50% inhibitory concentration, we calculated an IC_{50} values of 13.3 ± 0.76 µM at 24 h, 7.01 ± 0.3 µM at 48 h and 4.6 ± 0.19 µM at 72 h (Fig. 3A).

When the effect of the drug was evaluated in terms of ability to affect cell proliferation, we found that the IC_{50} was of 5.3 ± 0.55 µM (Fig. 3B). The study on MSC cycle, performed at 24 h of treatment with the concentration of 10 and 20 µM, confirmed a significant increase of subG0/G1, that is indicative of a significant cell mortality, whereas any specific block of cycle phase was observed (Fig. 3C, D). This information is of crucial importance to define the right conditions (dosage and time) for treating MSCs, allowing to incorporate and then the drug-release with a minimal acceptable cytotoxic effect, settled in 1 h of treatment of cells with 12.5 µM of drug.

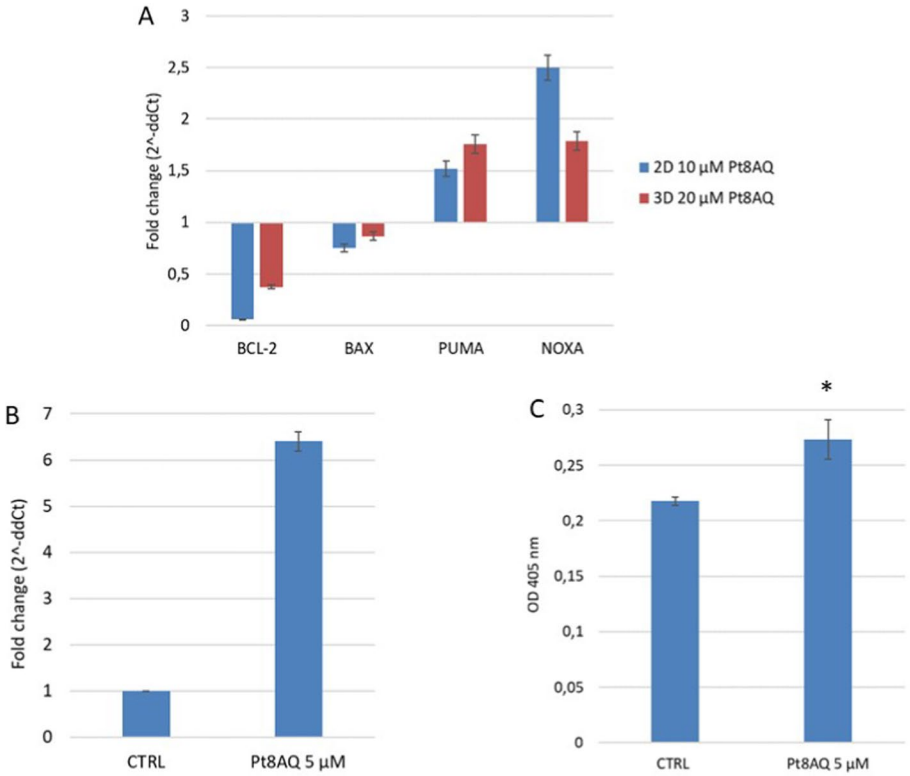

Fig. 2 Detection of pro-apoptotic molecules on U87-MG 3D spheroids treated with Pt-8AQ. **A** 2D versus 3D expression of BCL-2, PUMA, NOXA and BAX after 24 h of treatment with Pt-8AQ 5 µM (2D) or 20 µM (3D). The values are expressed as mean of two replicates. **B** RTq-PCR of proapoptotic molecules Caspase-3 on untreated U87-MG spheroids (CTRL) or treated 24 h with Pt-8AQ 5 µM. The values are expressed as mean of three replicates ± SEM. **C** Caspase-3 activity measurement after Pt-8AQ 5 µM treatment of spheroids (24 h). The histogram represents the optical density (OD) at 405 nm. Data are expressed as mean ± SEM of four replicates. (*$p < 0{,}001$)

Uptake and release of Pt-8AQ by MSCs

As reported above, the incorporation and release of Pt-8AQ by MSCs was performed by priming the cells with 12.5 µM of drug for 1 h. These conditions produced an acceptable number of viable cells (72% ± 10.2%) able to incorporate and then release the drug when the cells were cultured. After the drug priming, the amount of Pt-8AQ incorporated into MSCs (cell LYS) and measured by ICP–MS was found 0.91 ± 0.23 pg/cell. After 48 h of culture, the cells released 0.42 ± 0.03 pg/cell of platinum in their secretome, corresponding to a percentage of 46.76% out of the total drug incorporated (Fig. 4A).

The anticancer activity of the drug incorporated by MSCs (cell LYS) and the one present in the secretome, resulted in a higher dose dependent inhibition activity than the pure fresh drug(Fig. 4B). The comparison of the IC_{50} values evidenced a value of 499.5 ± 143.0 ng/ml for cell lysate and an IC_{50} of 406.7 ± 35.7 ng/ml for secretome, that were statistically significant lower ($p < 0{,}001$) than the fresh drug's value (1690.5 ± 89.7 pg/cell) (Fig. 4C).

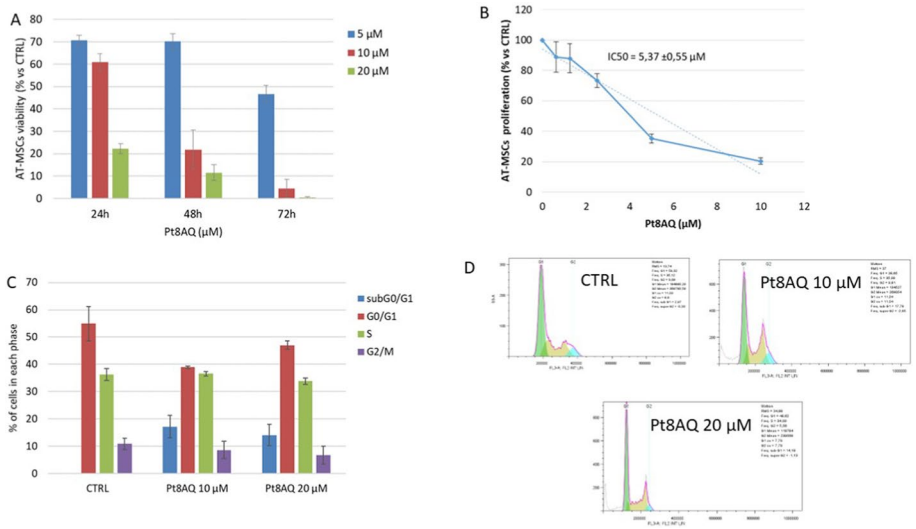

Fig. 3 In vitro activity and cell-cycle effects of Pt-8AQ on adipose tissue-derived AT-MSCs. **A** Cytotoxic activity of Pt-8AQ was evaluated after 24, 48 and 72 h of treatment with different concentrations of fresh drugs (from 5 to 20 µM) and expressed as cell viability (% of control cells). The table reports the IC_{50} values expressed as mean ± standard error (SEM) of six independent experiments. **B** Effect of increasing concentrations of Pt-8AQ was evaluated by a 7 day antiproliferation MTT assay on AT-MSCs. The effect was expressed as a percentage of the optical density measured in cultures that did not receive drugs (100% proliferation). **C** Histogram shows the effect of Pt-8AQ treatment (10 µM and 20 µM) on AT-MSCs after 24 h of treatment. The percentages of cells counted in each different cell phase (sub G0/G1, G0/G1, S and G2/M) are reported and compared to those found in untreated cells (CTRL). The values are expressed as mean ± standard error of five independent experiments. Two donors of AT-MSCs were used for the experiments. **D** Example of cell cycle analysis profile by flow cytometry

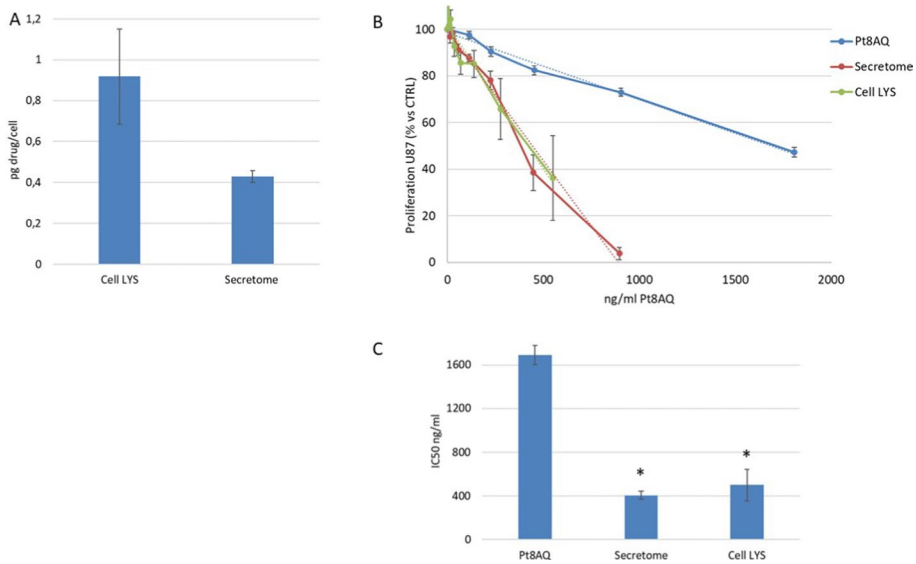

Fig. 4 In vitro activity of secretome and cell lysates from AT-MSCs loaded with Pt-8AQ 12,5 µM on U87-MG. **A** Pt-8AQ loaded by AT-MSCs upon 1 h of treatment with 12.5 µM of drug (cell LYS) and secreted in the medium upon 48 h of incubation (secretome), expressed by pg of drug per cell. **B** Activity of free drug, secretome and cell lysate on the proliferation of U87-MG. Data are expressed as percentage of cell growth normalized on the effect of secretome or lysate released by untreated AT-MSCs used as controls. Dotted lines represent linear regression of each curve. **C** Values of IC_{50} found for PT-8AQ, secretome, and lysates expressed in ng/ml of drug. In each graph, data are reported as the mean ± standard error of at least three independent experiments. (*$p < 0.001$)

Extracellular vesicles analyses of secretome

The NTA analyses of secretome of untreated (Fig. 5C) and Pt-8AQ loaded MSCs (Fig. 5D) showed the presence of EVs with a particle size ranging from 130 to 410 nm with a d50 of about 200 nm. The ζ-potential of the EVs ranged between − 16 and − 23 mV regardless the presence of Pt-8QA, in line with the values previously found with EVs deriving from the same cells. (Coccè et al. 2019) By evaluating the amount of Evs secreted by MSCs from three different donors, high variability was found, without any significant differences in secretion (Fig. 5B). In pellets of ultra-centrifuged secretome containing EVs and in their supernatant, the amount of Pt-8AQ was determined by ICP–MS, allowing to establish a proper dosage for the evaluation of their activity against U87-GM cells line (Fig. 5A).

Both whole secretome and supernatant produced a dose dependent inhibition with IC_{50} values of 406.7 ± 35.7 ng/ml and 414.2 ± 31.9 ng/ml, respectively, indicating a significant increasing in activity ($p < 0.001$), in comparison with the free fresh drug (IC_{50} 1690.5 ± 89.7). The dosage of Pt-8AQ in pellets containing EVs evidenced a very low amount of drug (about 10% of the detected in supernatants) and, of course, exerted a very poor anticancer activity (Fig. 5A). These data clearly suggest that the drug released by MSCs in the secretome is not associated with EVs.

The activity of drug present in secretome has also been confirmed on the U87-GM spheroids, if measured as ability to induce caspase-3 expression (Fig. 6A) and capability to affect cell viability, evaluated by MTT assay (Fig. 6B).

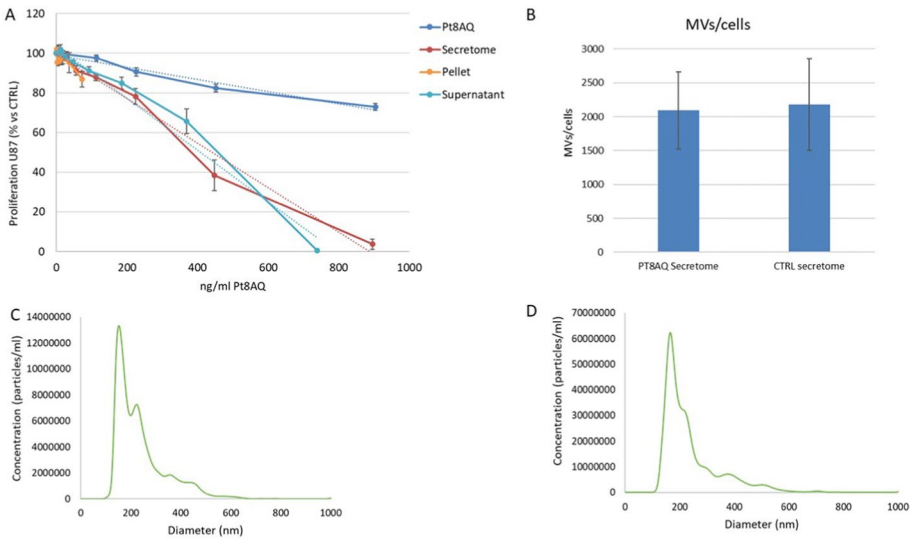

Fig. 5 *Antitumoral effect of MVs secreted by AT-MSCs loaded with Pt-8AQ.* **A** In vitro antiproliferative activity on U87-MG cell line of fresh drug, secretome, and MVs pellet isolated by ultracentrifugation (100000 g). The supernatant after centrifugation was also tested. Data are expressed as percentage of cell growth normalized on the effect of secretome, pellet, and supernatant obtained by untreated AT-MSCs. Dotted lines represent linear regression of each curve. Data are reported as the mean ± standard error of at least three independent experiments. **B** Number of MVs per cell counted in the secretome derived from Pt-8AQ-loaded AT-MSCs or control AT-MSCs. Data are reported as the mean ± standard error of at least three independent experiments. **C** and **D** Representative plot of size distribution analysis of the secretomes of AT-MSC©TRL **C** and AT-MSCs/Pt-8AQ **D** analyzed by nanoparticle tracking assay (NTA). In both samples, several populations of vesicles were present at 200—300 nm

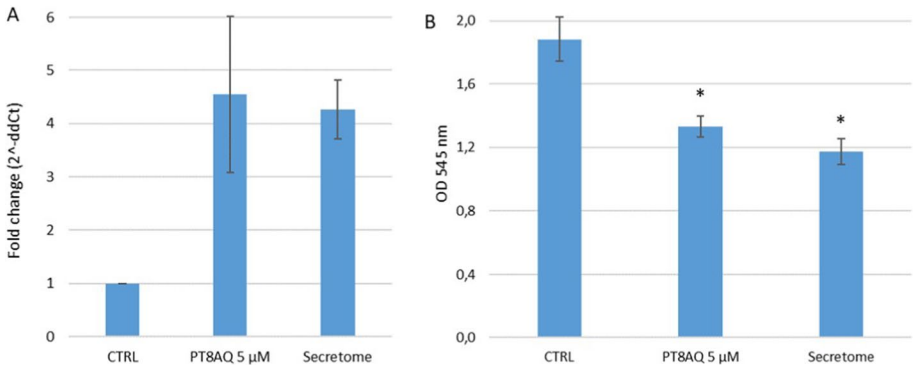

Fig. 6 Activity of AT-MSCs/Pt-8AQ secretome on U87-MG 3D spheroids. **A** RTq-PCR of Caspase-3 on untreated spheroids (CTRL) or treated 24 h with Pt-8AQ 5 µM or the secretome of AT-MSCs loaded with Pt-8AQ. The values are expressed as mean of three replicates ± SEM**. B** MTT assay on U87-MG spheroids treated 24 h with Pt-8AQ 5 µM or AT-MSCs/Pt-8AQ secretome, compared to untreated control spheroids. Data are expressed as optical density (OD) at 545 nm and are the mean ± SEM of three replicates

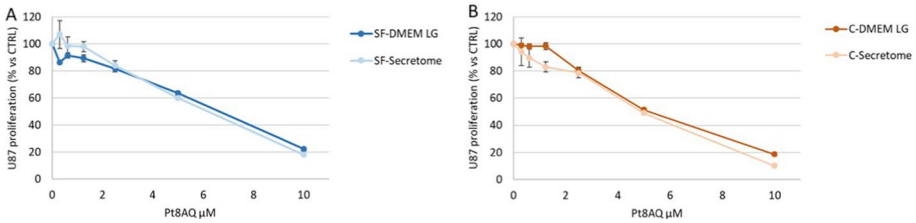

Fig. 7 Activity of Pt-8AQ on U87-MG cells. Pt-8AQ was dissolved in **A** serum-free medium (SF-DMEM LG) and serum-free secretome of untreated AT-MSCs (SF-secretome) or in **B** complete medium (C-DMEM LG) and complete secretome of untreated AT-MSCs (C-secretome)

Activity on U87-MG cells of Pt-8AQ dissolved in different conditions

Pt-8AQ dissolved in serum-free medium (SF-DMEM LG), serum-free secretome of untreated AT-MSCs (SF-secretome), complete medium (C-DMEM LG) and complete secretome (C-secretome) of untreated AT-MSCs showed an identical dose dependent inhibition of U87-MG proliferation, as evinced by the comparison between the calculated IC_{50} values ($p > 0.05$) (Fig. 7).

The activity of Pt-8AQ was evaluated by a 7-day antiproliferation MTT assay. The effect was expressed as a percentage of the optical density measured in cultures that did not receive drugs (100% proliferation). Data are reported as the mean ± standard error of at least three independent experiments.

Interaction between AT-MSCs and U87-MG spheroid in vitro

As expected, untreated MSCs significantly integrated with spheroid of U87-MG being able to proliferate. In addition, MSCs loaded with Pt-8AQ, although unable to proliferate, showed the ability to integrate into the 3D structure of U87-MG spheroids (Fig. 8).

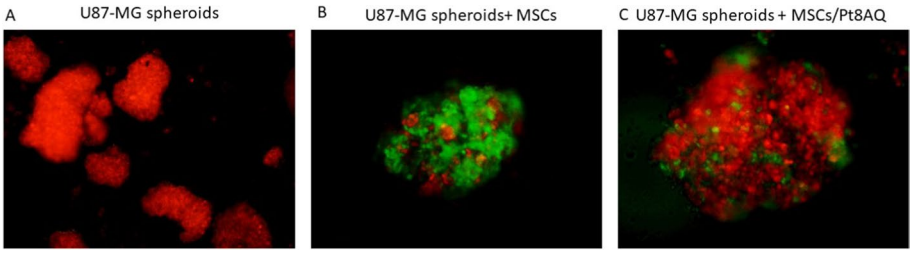

Fig. 8 Interaction between AT-MSCs and U87-MG spheroid in vitro. The interaction between MSCs and spheroids was evaluated by mixing fluorescent MSCs (hASCs-TS/GFP.$^{+}$) with U87-MG fluorescent spheroids (U87-MG RFP +) and further evaluated by fluorescence microscopy analysis. Representative images of: **A** U87-MG RFP + spheroids, **B** U87-MG RFP + spheroids and fluorescent MSCs (CTRL), or **C** after Pt-8AQ priming. (40 × magnification)

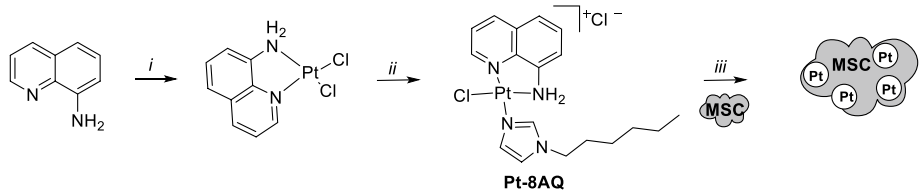

Scheme 1. Synthesis of Pt-8AQ and loading on MSCs**.** Reagents and Conditions: (i) K_2PtCl_4, H_2O/HCl 6 M (8 equiv.), reflux for 18 h; (ii) Alkyl-imidazole, DMF, 55 °C 18 h; (iii) DMEM, final concentration of 12.5 µM, 1 h at 37 °C

Discussion

In a previous study, we found that the new platinum metal complex Pt-8AQ was active in vitro against different types of tumors and expressed a significant efficacy, higher than CisPt, on human glioblastoma cell lines with different p53 gene expression. (Coccè et al. 2021; Facchetti et al. 2019).

Here, we confirmed our previous results in traditional 2D cell culture, demonstrating the anticancer activity of Pt-8AQ also against U87-GM cells grown as 3D multicellular spheroids. Dosages of 20 µM almost completely inhibited the spheroid formation and 5 µM of the drug produced a significant dramatic degradation after 96 h of treatment upon its addition to pre-formed spheroids (Fig. 1). The analysis of pro-apoptotic genes showed a reduced expression of BCL-2 and BAX together with an increase of PUMA and NOXA genes, with a gene profile expression identical as previously found with U87-GM cells cultured in 2D. The triggering of the apoptotic process has also been confirmed by the increase of caspase 3 expression and activity (Fig. 2). Since the 3D system somehow mimics the structure of a solid tumor, these observations may have translational value for predicting the significant efficacy of Pt-8AQ also in vivo tumor growth.

Being Pt-8AQ complex endowed with high chemical stability, we considered it for setting up incorporation and release procedures by MSCs for possible application in cell-mediated drug delivery systems (Scheme 1).

In fact, according to our previous experience with different anticancer molecules (Pessina et al. 2011) and also with a less stable platinum-based complex as CisPt, (Rimoldi et al. 2018) the MSC-based drug delivery system turned out an interesting and applicable new approach for cancer therapy. For this purpose, we have

preliminary investigated the MSCs sensitivity to Pt-8AQ and found that Pt-8AQ was able to block cell proliferation (IC_{50} 5.3 μM), as confirmed by the increased of subG0/G1 phase of cell cycle. Based on the 24 h cytotoxicity assay (Fig. 3), we selected the dosage of 12.5 μM and 1 h of treatment as optimal conditions for priming MSCs with Pt-8AQ.

These conditions furnished an acceptable number of viable cells, that have incorporated Pt-8AQ but still viable (cell Lys) with almost 50% of them able to release the drug after 48 h of culture. The anticancer activity of primed MSCs secretome on U87-GM proliferation demonstrated the drug release ability not only maintaining its activity but, surprisingly, increasing it when compared to the free drug (Fig. 4).

Since in our previous study we had demonstrated that other drugs (e.g., paclitaxel) incorporated by MSCs can be released with the drug encapsulated into exosome/extra cellular vesicles, (Pascucci et al. 2014; Crivelli et al. 2017; Luo et al. 2023; Yeo et al. 2013) we proceeded to analyze the amount and the size distribution of EVs in the secretome by NTA analyses. Furthermore, to see if the high activity of secretome was due to Pt-8AQ encapsulated into EVs, we isolated them by ultracentrifugation and measured the amount of the drug both in the pellets containing EVs and in the related supernatant. Despite the pellets contained about the 84% of the EVs present in the whole secretome, the amount of drug was only 9.6% while the found drug in the supernatant was over 90%. The different quantitative distribution of the drug between EVs pellets and the supernatant was clearly confirmed by the anticancer efficacy. These results undoubtedly suggested that Evs are not the main pathway used by MSCs to release the incorporate drug. As stated above, the highest and almost total Pt-8AQ concentration could be measured the supernatant even if it still remains to explain the discrepancy between the higher activity of Pt-8AQ secreted by MSCs respecting to the fresh free Pt-8AQ. To verify a possible synergism of factors released by MSCs, i.e., citokine/chemokine or miRNA, between the drug and serum proteins, we investigated the activity of Pt-8AQ both when dissolved in complete medium, in serum free medium or into secretome of untreated MSCs (Fig. 7).

These results not only, established that secretome of MSCs did not exert "per se" any anticancer activity on U87-GM cells, but indeed confirmed that Pt-8AQ did not modify its activity under the different conditions tested, taken into consideration it cannot be excluded, however, that the MSCs might have modified their secretome in response of Pt-8AQ priming and released the drug bound to some carrier able to enhance the drug bioavailability. it is worth nothing actually that the exact mechanism of action of this new Pt-drug has not completely been elucidated, although already proved not be attributed to DNA adducts formation. However, considering the previously demonstrated Pt-8AQ ability to bind RNAse, we might no exclude some cytotoxic mechanism related to protein synthesis. (Sacco et al. 2021) In our model, if the drug was effectively released bound to RNAse we could hypothesize a possible contribution of this new formed adduct to increase both the drug bioavailability and activity on cancer cells. Further proteomic investigation will be realized to identify the possible species involved in drug activity, with the aim to clarify its mechanism of action as much as possible.

It is worth nothing indeed that MSCs/Pt-8AQ secretome was demonstrated active also on spheroids as proved both by the increased caspase 3 expression and activity

and the decreased cancer cells viability, suggesting the activation of apoptotic mechanisms (Fig. 6).

Up today, many attempts have been realized to overcome systemic toxicity, using locally advanced therapy, in particular with those treatments that have shown drug dose as limiting factor. (Enríquez Pérez et al. 2019) Therefore, in the perspective to use MSCs in situ for the treatment of glioblastoma, we verified the level of interaction between MSCs and U87-MG cancer cells by mixing spheroid from U87-RFP + (red) with MSC-GFP + (green) to highlight if MSCs were able both to adhere and to be integrated into the spheroids (Fig. 8). As reported in our previous studies (Pacioni et al. 2017) MSCs are able to migrate to and colonize GBM tumor xenografts both when injected directly into the brain and when systemically administered. Furthermore, they are "per se" able to affect tumor growth in orthotopic glioblastoma xenografts. Based on this tropism of MSCs toward brain tumors, we can suppose that MSCs primed with Pt-8AQ can be integrated within the tumor mass and release the drug, producing a local high anticancer efficacy with a reduction of systemic toxicity and side effects.

By mimicking a possible in vivo and in situ treatment of GBM having a mass of 20 cm^3 with Pt-8AQ loaded in MSCs, we could estimate that 30×10^6 cells, that might be easy to inject in a very small volume, could indeed deliver about 27 μg of Pt-8AQ corresponding to an *in-situ* concentration of about 1350 ng/ml equivalent to three time the IC_{50} value. As the use of MSCs is considered sometimes controversial, we should note that, in such a delivery system, the MSCs are in pre-apoptotic phase and in a final step of their life and thus compatible with high safety conditions.

Conclusions

Drug delivery systems by MSCs is classified by regulatory agency as advanced therapy medicinal products (ATMPs) that can also be supported by large-scale production in bioreactor. (Lisini et al. 2020) Cells loaded with Pt-8AQ could provide a potential approach to facilitate the GMB therapy by intra-tumoral administration of cells, able to integrate them into the tumor mass and thus exerting high therapeutic efficacy in situ. The increased efficacy found for the Pt-8AQ delivered by MSCs even suggested to deeper investigate a possible direct use of MSCs secretome both in situ and/or by systemic administration, being secretome able to cross the blood–brain tumor. MSC-based cell therapies could furnish new possible important adjuvant tools in addition to conventional treatments based on surgery, radiotherapy and traditional chemotherapy.

Methods

Drug

Pt-8AQ (caPt(II) complex) (Facchetti et al. 2019) was prepared at a concentration of 4 mg/mL (7.112 μM) in dimethyl sulfoxide (DMSO; Sigma-Aldrich, St. Louis, Missouri, USA) and working solutions were freshly prepared according to the experimental design by serial dilutions in complete culture medium. (Coccè et al. 2021).

Tumor cell line

Both glioblastoma cell line U87-MG, (Fogh et al. 1977) and U87-MG expressing red fluorescent protein (U87-MG RFP +) were used. Tumor cells were maintained by 1:5 weekly

dilution in DMEM LG medium supplemented with 10% FBS and 2 mM L-glutamine and incubated at 37 °C, 5% CO_2. All reagents for cell cultures were provided by Euroclone (Pero MI, Italy).

3D multicellular cultures of U87-MG

3D multicellular tumor spheroids were prepared as described previously. (Roncoroni et al. 2008) Briefly, cultures were initiated by seeding 2.5×10^5 cells/ml in 13 ml of complete Iscove modified Dulbecco's medium (Euroclone) + 10% FBS (Euroclone) in polycarbonate Erlenmeyer flasks (Euroclone) incubated in a gyratory incubator (Colaver, Milan, Italy) at 60 rev/min at 37 °C in air atmosphere. Homotypical aggregations, visible after 3 days of culture, were usually complete within 5 days. To study the effect of 5, 10 and 20 μM Pt-8AQ on spheroid formation the drug was added at time zero together with cells and collected after 6 days. To study the effect of preformed spheroids, the drug was added to 3D tumor cell aggregates at sixth day at concentrations of 10 and 20 μM and kept in the incubator for additional 24 h. Control cultures received the same volume of medium.

Mesenchymal stromal cells

Mesenchymal stromal cells were obtained from adipose tissue lipoaspirates from adult donors collected after written informed consent in accordance with the Declaration of Helsinki and the approval of the Institutional Ethical Committee of IRCCS C`a Granda Ospedale Maggiore Policlinico of Milan (#978). The cells isolation was obtained by enzymatic digestion and the expansion and characterization of MSCs was performed according to the previously described procedure. (Coccè et al. 2021; Ceserani et al. 2016) Adipose tissue-derived mesenchymal stromal cells (AT-MSCs) from three different donors were used for loading Pt-8AQ. Cells were expanded in 25 cm^2 flasks at a density of 1.2×10^4 cells/cm^2 in 5 mL of Dulbecco's modified Eagle's medium (DMEM LG) supplemented with 5% platelet lysate Stemulate (Cook Regentec, Indianapolis, IN, USA) and 2 mM L-glutamine and incubated at 37 °C, 5% CO_2.(Lisini et al. 2020) To study cancer cells MSCs interaction was used an immortalized cell line of AT-MSCs expressing the green fluorescent protein (hASCs-TS GFP +) cultured in DMEM LG + 10% fetal bovine serum (FBS) + 2 mM L-glutamine.(Coccè et al. 2017).

Cytotoxicity and antiproliferation assays on MSCs

Since AT-MSCs were used as drug delivery cells for Pt-8AQ, cytotoxic effects of the drug on stem cells were evaluated as follows. AT-MSCs were seeded in 96-well plates (15,000 cells/well) and incubated for 24 h in complete medium. Then, cells were treated with increasing concentration of Pt-8AQ (5, 10, 20 μM) and incubated at 37 °C, with 5% CO_2 for 24, 48 or 72 h. Cell viability was evaluated by MTT (3-(4,5-dimethyl-2-thiazolyl)-2,5-diphenyl-2-H-tetrazoliumbromide) assay, as previously described.(Pessina et al. 2011) Antiproliferative activity of Pt-8AQ on mesenchymal cells was also assayed by seeding 4000 cells/well in 96-well plates in the presence of increasing doubling concentrations of the drug (from 0.625 to 10 μM). After 7 days of incubation in growing conditions, cell viability was tested by MTT assay. The inhibitory concentration (IC_{50}) was

determined applying the Reed and Muench formula (Reed 1938) using Excel (Microsoft, Inc).

Cell cycle assay

To analyze the cell cycle of AT-MSCs after the treatment with 0 (CTRL), 10, and 20 μM Pt-8AQ, AT-MSCs were seeded at concentration of 20,000 cells/cm^2 in 6-multiwell plates. After 24 h of drug treatment (37 °C, 5% CO_2), cells were suspended in phosphate-buffered saline (PBS) and fixed with 70% (v/v) ethanol for 1 h at 4 °C. Upon a further PBS wash, cells were suspended in propidium iodide 50 μg/mL in PBS. Cells were incubated overnight at 4 °C and analyzed by flow cytometry (Navios EX, Beckman Coulter, Brea, CA, USA). At least 10^4 events per sample were acquired and analyzed using a specific software (Navios EX Softwar, Beckman Coulter). Data are expressed as the mean fluorescence intensity (MFI) of the specific antibody.

Real-time PCR analyses

Total RNA was extracted from spheroids of U87-MG treated with Pt-8AQ (5 μM, 10 μM) for 24 h following instructions of PureLink™ RNA Mini Kit (Thermofisher scientific, Waltham, Massachusetts, USA). RNA was treated with DNase to exclude DNA contamination, and then, 1 μg of RNA was reverse-transcribed into cDNA using a QuantiTect Reverse Transcription Kit (Qiagen, Hilden, Germany). Samples were analyzed using real-time quantitative PCR (RT-qPCR). PCR reactions were performed using Rotor-Gene Q cycler (Qiagen), and the amplifications were carried out using the QuantiNova™ SYBR® Green PCR (Qiagen) in a total volume of 20 μL. Real-time PCR was performed using the following primer sequences (5′–3′, Ta = 60 °C):

Gene target	Accession Number	Forward sequence	Reverse sequence
GAPDH	NM_001289745	GGAGTCAACGGATTTGGTCG	CTTCCCGTTCTCAGCCTTGA
NOXA	NM_001382617	GCTGGAAGTCGAGTGTGCTA	GGAGTCCCCTCATGCAAGTT
BCL2	NM_000633	ATCGCCCTGTGGATGACTGAGT	GCCAGGAGAAATCAAACAGAGGC
PUMA	NM_014417	ATGCCTGCCTCACCTTCATC	TCAGCCAAAATCTCCCACCC
BAX	NM_001291429	TGGCAGCTGACATGTTTTCTGAC	TCACCCAACCACCCTGGTCTT
CASPASE-3	NM_001354783	ATTTGGAACCAAAGATCATACATGG	TTCCCTGAGGTTTGCTGCAT

Data were analyzed by using the $2^{-\Delta\Delta Ct}$ method to obtain the relative expression level, and each sample was normalized by using GAPDH RNA expression. The experiments were carried out in duplicate, and each data reports the mean value.

Drug loading of MSCs

Mesenchymal stem cells were loaded with Pt-8AQ following a previous described procedures with little modifications. (Pessina et al. 2011) Sub-confluent cultures of AT-MSCs (around 2×10^4 cells/cm^2) were treated at for 2 h at 37 °C with Pt-8AQ at a final concentration of 12.5 μM. After drug priming, the adherent cells were washed twice with PBS, detached by trypsin and washed twice at 600xg for 10 min in Hank's solution (HBSS, Euroclone UK). To determine the amount of drug internalized by stromal cells (cell-lys), an aliquot of 1×10^6 was collected and lysed by three sonication cycles of 0.4 s pulse cycle and 30% amplitude (Labsonic U Braun). The primed

cells were resuspended in 5 ml of DMEM without serum and seeded in 25 cm^2 flasks to release the drug in the secretome. The same amount of unprimed AT-MSCs was seeded in 25 cm^2 flasks, 5 ml of culture medium and their secretome were used as control. The conditioned media of control (CM/CTRL) and Pt-8AQ-treated MSCs (CM/Pt-8AQ) were collected after 48 h of incubation (37 °C, 5% CO_2). Cell lysates and CM of control and Pt-8AQ-treated AT-MSCs were tested on U87-MG cell line in a 7-day proliferation assay, and cell viability was assessed by MTT assay.

Determination of Pt-8AQ concentration

Both the lysates (LYS/Pt-8AQ) and the conditioned media (CM 48 h Pt-8AQ) were dissolved in 1% HNO_3. Platinum was quantified by inductively coupled plasma mass spectrometry (ICP–MS) (BRUKER aurora M90 ICP–MS, MA, USA) according to the previously described method. (Ferri et al. 2013) Cellular metal levels were expressed as the mean of three independent determinations as µg Pt per L of lysate or medium. The amount of Pt was transformed into Pt-8AQ, through this formula:

$$\mathrm{Pt-8AQ} = \frac{\left(\mathrm{Pt}\frac{\mathrm{g}}{\mathrm{L}}\right)}{\mathrm{MW\ Pt}\left(\frac{\mathrm{g}}{\mathrm{mol}}\right)} \times \mathrm{MW\ Pt-8AQ}\left(\frac{\mathrm{g}}{\mathrm{mol}}\right)$$

The concentration found (ng/ml) of Pt-8AQ was then evaluated as picoMolar per single AT-MSCs.

The inhibitory effect of CM and cell lysates from drug loaded AT-MSCs were evaluated on U87-MG proliferation by the MTT assay, and the inhibitory concentration IC_{50} was determined according to the Reed and Muench formula. (Reed 1938) The anti-tumoral activity of CM 48 h/Pt-8AQ, LYS pre-release/Pt-8AQ, LYS post-release/Pt-8AQ were compared to Pt-8AQ quantification obtained by inductively coupled plasma mass spectrometry (ICP–MS).

Extracellular vesicles analysis

The conditioned media of control (CM/CTRL) and Pt-8AQ-treated MSCs (CM/Pt-8AQ) collected after 48 h of incubation (37 °C, 5% CO_2) were also used to quantify the presence of extracellular vesicles (EVs) and their physico-chemical characterization. Particles size distribution and concentration of EVs were studied by Nanoparticles Tracking Analysis (NTA) using a Nanosight NS300 (Malvern Instrument, Malvern, Worcestershire, UK), equipped with a blue laser and a sCMOS camera. NTA was performed after diluting samples in ultrapure water recording for each sample 5 videos of 60 s that were subsequently analyzed using NTA software 3.0. The ζ-potential of the samples was instead measured by using a Zetasizer (Nano-ZS, Malvern Instrument, Malvern, Worcestershire, UK) after 1:4 dilution of the sample in ultrapure water. The results are the mean of three independent measurements. The Evs in secretome were purified by ultracentrifugation using an Optima TL Ultracentrifuge at 100,000×G for 2.5 h. Both the supernatants and the pellets (resuspended in DMEM) were analyzed for the Pt-8AQ dosage and anticancer activity as above described.

Activity of Pt-8AQ dissolved in different conditions on U87-MG cells

The effect of Pt-8AQ against U87-MG cell proliferation has been studied in 96 multiwell plates (Sarstedt, Nümbrecht, Germany). Pt-8AQ was dissolved in serum-free medium (SF-DMEM LG), serum-free secretome of untreated AT-MSCs (SF-secretome), complete medium (C-DMEM LG) and complete secretome (C-secretome) of untreated AT-MSCs. Briefly, 1:2 serial dilutions of pure drug (from 0.27 ± 35.52 µM Pt-8AQ) were prepared in 100 µL of medium per well, and then to each well, has been added 2000 tumor U87-MG cells. After 7 days of culture (anti-proliferative assay) at 37 °C and 5% CO_2, cell growth was evaluated by MTT assay (3-(4,5-dimethyl-2-thiazolyl)-2,5-diphenyl-2-H-tetrazolium), as previously described. (Coccè et al. 2021) The inhibitory concentration (IC50) was determined by applying the Reed and Muench formula (Reed 1938) using Excel (Microsoft, Inc, Albuquerque, NM, USA).

Interaction between AT-MSCs and U87-MG spheroid in vitro

To study the interaction between U87-MG spheroids and mesenchymal stromal cells, U87-MG spheroids obtained by cells that expressed red fluorescent protein (U87-MG RFP +) were co-cultured with fluorescent MSCs (hASCs-TS/GFP +) that were previously established in our laboratory. (Cocce et al. 2017) Briefly, U87-MG spheroids were co-cultured with MSCs both untreated or primed with Pt-8AQ (at ratio 5:1 spheroids/MSCs). After 24 h of incubation the MSCs cells integrations in spheroids was analyzed under a fluorescent microscope.

Statistical analysis

Data are expressed as average ± standard deviation (SD). Differences between mean values were evaluated according to Tukey–Kramer Multiple Comparisons Test performed by GRAPHPADINSTAT program (GraphPad Software Inc., San Diego, CA, USA). p values ≤ 0.05 were considered statistically significant. The linearity of response and the correlation were studied using regression analysis, by Excel 2019 software (Microsoft, Inc.)

Abbreviations

ATMP	Advanced therapy medicinal products
AT-MSCs	Adipose-tissue mesenchymal stromal cells
BBB	Blood–brain barrier
CisPt	Cisplatin
CM	Conditioned media
DMEM LG	*Dulbecco's modified eagle medium* low glucose
DMSO	Dimethyl sulfoxide
EVs	Extracellular vesicles
FBS	Fetal bovine serum
GBM	Glioblastoma multiforme
GFP	Green fluorescent protein
ICP–MS	Inductively coupled plasma mass spectrometry
LYS	Lysate
MFI	Mean fluorescence intensity
MSCs	Mesenchymal stromal cells
MTT	3-(4,5-Dimethyl-2-thiazolyl)-2,5-diphenyl-2-H-tetrazoliumbromide
NTA	Nanoparticles tracking analysis
O^6-BG	O^6-benzylguanine
PBS	Phosphate-buffered saline
Pt-8AQ	Cationic platinum(II) complex bearing 8-aminoquinoline as chelating ligand
RFP	Red fluorescent protein

SF Serum-free
TMZ Temozolomide

Acknowledgements
The authors acknowledge the support of the APC central fund of the University of Milan.

Author contributions
VC: data curation, investigation, formal analysis. EM: data curation, formal analysis, investigation. LD: data curation, formal analysis, IR: supervision, writing—review and editing GF: validation, writing—review and editing. GC: data curation, formal analysis. GL: data curation LR: investigation, AG and CC: funding acquisition. GA: data curation, resources. EC: investigation FC: data curation. SF: data curation, formal analysis. FP: SUPERVISION, investigation. AP: conceptualization, project administration, writing—original draft. All the authors read and approved the final manuscript.

Funding
This study was supported by funds from University of Milan-Piano di sostegno alla Ricerca 2022-LINEA 2.

Availability of data and materials
Data will be made available on request.

Declarations

Ethics approval and consent to participate
Not applicable.

Consent for publication
Not applicable.

Competing interests
The authors declare that they have no competing interests.

Author details
[1]CRC StaMeTec, Department of Biomedical, Surgical and Dental Sciences, University of Milan, 20122 Milan, Italy. [2]CRC StaMeTec, Department of Pharmaceutical Science, University of Milan, Via Mangiagalli 25, 20133 Milan, Italy. [3]Department of Agricultural and Environmental Sciences - Production, Landscape, Agroenergy, Via Celoria 2, 20133 Milano, Italy. [4]CRC StaMeTec, Department of Biomedical, Surgical and Dental Sciences, University of Milan, 20122 Milan, Italy. [5]Center for Prevention and Diagnosis of Celiac Disease, Gastroenterology and Endoscopy Unit, Fondazione IRCCS Ca' Granda Ospedale Maggiore Policlinico, 20122 Milan, Italy. [6]Maxillo-Facial and Dental Unit, Fondazione Ca' Granda IRCCS Ospedale Maggiore Policlinico, 20122 Milan, Italy. [7]Department of Biomedical Surgical and Dental Sciences, Sports Trauma Researches Center, University of Milan c/o 1st Division of Orthopedics and Traumatology, Orthopedic Center Pini CTO - ASST Gaetano Pini, Milan, Italy. [8]Laboratory of Clinical Pathology and Medical Genetics, Istituto Neurologico Fondazione C. Besta, Milan, Italy. [9]Department of Diagnostics and Technology, Fondazione IRCCS Istituto Neurologico "C. Besta", Milano, Italy.

Received: 21 September 2023 Accepted: 20 December 2023
Published online: 10 January 2024

References

Alessandri G, Chirivi RGS, Fiorentini S, Dossi R, Bonardelli S, Giulini SM, Zanetta G, Landoni F, Graziotti PP, Turano A et al (1999) Phenotypic and functional characteristics of tumour-derived microvascular endothelial cells. Clin Exp Metas 17(8):655–662

Bonomi A, Coccè V, Cavicchini L, Sisto F, Dossena M, Balzarini P, Portolani N, Ciusani E, Parati E, Alessandri G et al (2013) Adipose tissue-derived stromal cells primed in vitro with paclitaxel acquire anti-tumor activity. Int J Immunopathol Pharmacol 26(1 Suppl):33–41

Ceserani V, Ferri A, Berenzi A, Benetti A, Ciusani E, Pascucci L, Bazzucchi C, Coccè V, Bonomi A, Pessina A et al (2016) Angiogenic and anti-inflammatory properties of micro-fragmented fat tissue and its derived mesenchymal stromal. Cells. https://doi.org/10.1186/s13221-016-0037-3

Chernov AN, Alaverdian DA, Galimova ES, Renieri A, Frullanti E, Meloni I, Shamova OV (2021) The phenomenon of multidrug resistance in glioblastomas. Hematol Oncol Stem Cell Ther. https://doi.org/10.1016/j.hemonc.2021.05.006

Coccè V, Farronato D, Brini AT, Masia C, Giannì AB, Piovani G, Sisto F, Alessandri G, Angiero F, Pessina A (2017) Drug loaded gingival mesenchymal stromal cells (GinPa-MSCs) inhibit in vitro proliferation of oral squamous cell carcinoma. Sci Rep 7(1):9376

Coccè V, Franzè S, Brini AT, Giannì AB, Pascucci L, Ciusani E, Alessandri G, Farronato G, Cavicchini L, Sordi V et al (2019) In vitro anticancer activity of extracellular vesicles (EVs) secreted by gingival mesenchymal stromal cells primed with paclitaxel. Pharmaceutics. https://doi.org/10.3390/pharmaceutics11020061

Coccè V, Rimoldi I, Facchetti G, Ciusani E, Alessandri G, Signorini L, Sisto F, Giannì A, Paino F, Pessina A (2021) In vitro activity of monofunctional pt-ii complex based on 8-aminoquinoline against human glioblastoma. Pharmaceutics 13(12):2101

Cocce V, Balducci L, Falchetti ML, Pascucci L, Ciusani E, Brini AT, Sisto F, Piovani G, Alessandri G, Parati E et al (2017) Fluorescent immortalized human adipose derived stromal cells (hASCs-TS/GFP+) for studying cell drug delivery mediated by microvesicles. Anticancer Agents Med Chem 17(11):1578–1585

Cordani N, Lisini D, Coccè V, Paglia G, Meanti R, Cerrito MG, Tettamanti P, Bonaffini L, Paino F, Alessandri G et al (2023) Conditioned medium of mesenchymal stromal cells loaded with paclitaxel is effective in preclinical models of triple-negative breast cancer (TNBC). Int J Mol Sci 24(6):5864

Crivelli B, Chlapanidas T, Perteghella S, Lucarelli E, Pascucci L, Brini AT, Ferrero I, Marazzi M, Pessina A, Torre ML (2017) Mesenchymal stem/stromal cell extracellular vesicles: from active principle to next generation drug delivery system. J Control Release 262:104–117
Damato AR, Luo J, Katumba RGN, Talcott GR, Rubin JB, Herzog ED, Campian JL (2021) Temozolomide chronotherapy in patients with glioblastoma: a retrospective single-institute study. Neuro-Oncol Adv. https://doi.org/10.1093/noajnl/vdab041
Enríquez Pérez J, Fritzell S, Kopecky J, Visse E, Darabi A, Siesjö P (2019) The effect of locally delivered cisplatin is dependent on an intact immune function in an experimental glioma model. Sci Rep 9(1):5632
Eramo A, Ricci-Vitiani L, Zeuner A, Pallini R, Lotti F, Sette G (2006) Chemotherapy resistance of glioblastoma stem cells. Cell Death Differ. https://doi.org/10.1038/sj.cdd.4401872
Facchetti G, Ferri N, Lupo MG, Giorgio L, Rimoldi I (2019) Monofunctional PtII complexes based on 8-aminoquinoline: synthesis and pharmacological characterization. Eur J Inorg Chem 2019(29):3389–3395
Ferri N, Cazzaniga S, Mazzarella L, Curigliano G, Lucchini G, Zerla D, Gandolfi R, Facchetti G, Pellizzoni M, Rimoldi I (2013) Cytotoxic effect of (1-methyl-1H-imidazol-2-yl)-methanamine and its derivatives in PtII complexes on human carcinoma cell lines: a comparative study with cisplatin. Bioorg Med Chem 21(8):2379–2386
Fogh J, Fogh JM, Orfeo T (1977) One hundred and twenty-seven cultured human tumor cell lines producing tumors in nude mice. J Natl Cancer Inst 59(1):221–226
Galli R, Binda E, Orfanelli U, Cipelletti B, Gritti A, Vitis S (2004) Isolation and characterization of tumorigenic, stem-like neural precursors from human glioblastoma. Cancer Res. https://doi.org/10.1158/0008-5472.CAN-04-1364
Hosseinalizadeh H, Mahmoodpour M, Razaghi Bahabadi Z, Hamblin MR, Mirzaei H (2022) Neutrophil mediated drug delivery for targeted glioblastoma therapy: a comprehensive review. Biomed Pharmacother 156:113841
Lee SY (2016) Temozolomide resistance in glioblastoma multiforme. Genes Dis 3(3):198–210
Lisa O, Lisenn L, Céline S, Dominique H, Pierre François C, François MV (2020) Drug resistance in glioblastoma: are persisters the key to therapy? Cancer Drug Resistance 3(3):287–301
Lisini D, Nava S, Frigerio S, Pogliani S, Maronati G, Marcianti A, Coccè V, Bondiolotti G, Cavicchini L, Paino F et al (2020) Automated large-scale production of paclitaxel loaded mesenchymal stromal cells for cell therapy applications. Pharmaceutics 12(5):411. https://doi.org/10.3390/pharmaceutics12050411
Luo H, Jin J, Jin J, Lou K, He H, Feng S, Zeng F, Zou J (2023) Emerging applications of extracellular vesicles in tumor therapy. Cancer Nanotechnology 14(1):63
Pacioni S, D'Alessandris QG, Giannetti S, Morgante L, Coccè V, Bonomi A, Buccarelli M, Pascucci L, Alessandri G, Pessina A et al (2017) Human mesenchymal stromal cells inhibit tumor growth in orthotopic glioblastoma xenografts. Stem Cell Res Ther 8(1):53
Pascucci L, Coccè V, Bonomi A, Ami D, Ceccarelli P, Ciusani E, Viganò L, Locatelli A, Sisto F, Doglia SM et al (2014) Paclitaxel is incorporated by mesenchymal stromal cells and released in exosomes that inhibit in vitro tumor growth: a new approach for drug delivery. J Control Release 192:262–270
Pessina A, Bonomi A, Coccè V, Invernici G, Navone S, Cavicchini L, Sisto F, Ferrari M, Viganò L, Locatelli A et al (2011) Mesenchymal stromal cells primed with paclitaxel provide a new approach for cancer therapy. PLoS One 6(12):e28321
Pessina A, Leonetti C, Artuso S, Benetti A, Dessy E, Pascucci L, Passeri D, Orlandi A, Berenzi A, Bonomi A et al (2015) Drug-releasing mesenchymal cells strongly suppress B16 lung metastasis in a syngeneic murine model. J Experim Clin Cancer Res 34(1):82
Reed MH (1938) A simple method of estimating fifty per cent endpoints. Am J Epidemiol 27(3):493–497
Rimoldi I, Coccè V, Facchetti G, Alessandri G, Brini AT, Sisto F, Parati E, Cavicchini L, Lucchini G, Petrella F et al (2018) Uptake-release by MSCs of a cationic platinum(II) complex active in vitro on human malignant cancer cell lines. Biomed Pharmacother 108:111–118
Roberts NB, Wadajkar AS, Winkles JA, Davila E, Kim AJ, Woodworth GF (2016) Repurposing platinum-based chemotherapies for multi-modal treatment of glioblastoma. Oncolmmunology 5(9):1208876
Roncoroni L, Elli L, Dolfini E, Erba E, Dogliotti E, Terrani C, Doneda L, Grimoldi MG, Bardella MT (2008) Resveratrol inhibits cell growth in a human cholangiocarcinoma cell line. Liver Int 28(10):1426–1436
Sacco F, Tarchi M, Ferraro G, Merlino A, Facchetti G, Rimoldi I, Messori L, Massai L (2021) Reactions with proteins of three novel anticancer platinum(II) complexes bearing n-heterocyclic ligands. Int J Mol Sci 22(19):10551
Sancho-Albero M, Facchetti G, Panini N, Meroni M, Bello E, Rimoldi I, Zucchetti M, Frapolli R, De Cola L (2023) Enhancing Pt (IV) complexes anticancer activity upon encapsulation in stimuli responsive nanocages. Adv Healthcare Mater. https://doi.org/10.1002/adhm.202202932
Singh N, Miner A, Hennis L, Mittal S (2021) Mechanisms of temozolomide resistance in glioblastoma—a comprehensive review. Cancer Drug Resist 4(1):17–43
Tan S, Wu T, Zhang D, Zhang Z (2015) Cell or cell membrane-based drug delivery systems. Theranostics 5(8):863–881
Tran C, Damaser MS (2015) Stem cells as drug delivery methods: application of stem cell secretome for regeneration. Adv Drug Deliv Rev 82–83:1–11
Wang Q, Hu B, Hu X, Kim H, Squatrito M, Scarpace L, deCarvalho AC, Lyu S, Li P, Li Y et al (2017) Tumor evolution of glioma-intrinsic gene expression subtypes associates with immunological changes in the microenvironment. Cancer Cell 32(1):42-56.e46
Wang C, Li K, Li T, Chen Z, Wen Y, Liu X, Jia X, Zhang Y, Xu Y, Han M et al (2018) Monocyte-mediated chemotherapy drug delivery in glioblastoma. Nanomedicine 13(2):157–178
Wu D, Chen Q, Chen X, Han F, Chen Z, Wang Y (2023) The blood–brain barrier: structure, regulation, and drug delivery. Signal TransductTargeted Ther 8(1):217
Yeo RW, Lai RC, Zhang B, Tan SS, Yin Y, Teh BJ, Lim SK (2013) Mesenchymal stem cell: an efficient mass producer of exosomes for drug delivery. Adv Drug Deliv Rev 65(3):336–341

Publisher's Note